nanomaterials

Supplementary Material

Plasma Ag-Modified α-Fe_2O_3/g-C_3N_4 Self-Assembled S-Scheme Heterojunctions with Enhanced Photothermal-Photocatalytic-Fenton Performances

Yawei Xiao [1], Bo Yao [1], Zhezhe Wang [1], Ting Chen [2,*], Xuechun Xiao [1,*] and Yude Wang [3,*]

[1] National Center for International Research on Photoelectric and Energy Materials, School of Materials and Energy, Yunnan University, Kunming 6500504, China
[2] Institute of Materials Science & Devices, School of Materials Science and Engineering, Suzhou University of Science and Technology, Suzhou, 215009, China
[3] Yunnan Key Laboratory of Carbon Neutrality and Green Low-Carbon Technologies, Yunnan University, Kunming 6500504, China
* Correspondence: chenting@mail.usts.edu.cn (T.C.); xchxiao@ynu.edu.cn (X.X.); ydwang@ynu.edu.cn (Y.W.)

Materials

Melamine ($C_3H_6N_6$, AR, ≥99.9%), Cyanuric acid ($C_3H_3N_3O_3$, AR, ≥99.9%), Iron(III) chloride hexahydrate ($FeCl_3·6H_2O$, AR, ≥99.9%), Silver nitrate ($AgNO_3$, AR, ≥99.9%), Sodium acetate (CH_3COONa, AR, ≥99.9%) were purchased from Aladdin Reagent (Shanghai) Co. Ltd, China. Ethanol absolute (C_2H_6O, ≥99.5%) was purchased from Shanghai Maclean Biochemical Technology Co. Ltd, China. All chemicals were sourced from commercial suppliers and were not further purified before being used, and deionized water was used throughout the experiments.

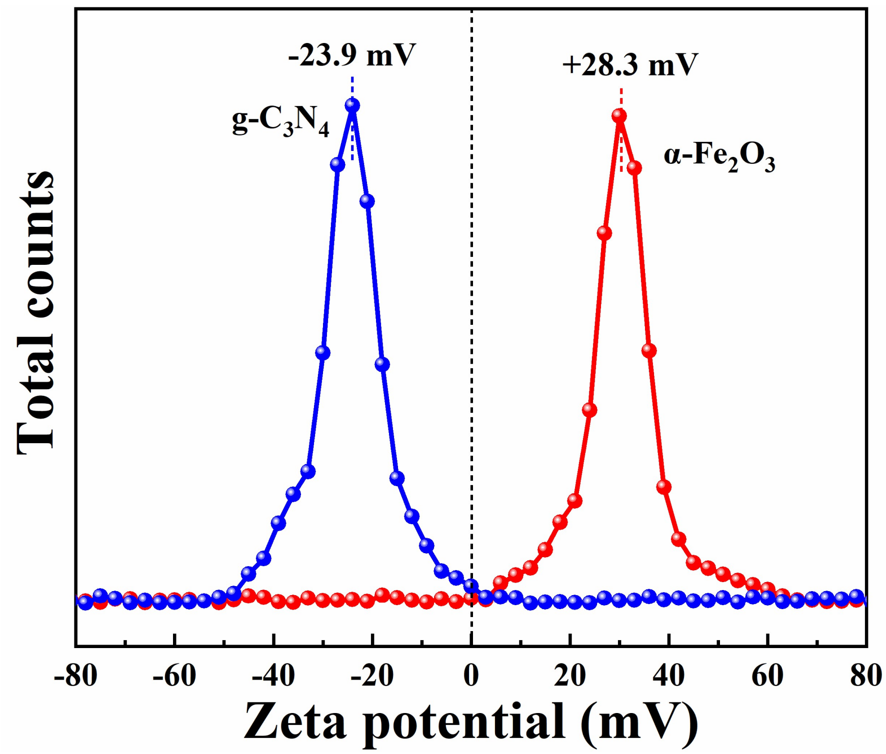

Figure S1. Zeta potential of the g-C_3N_4 and acidified α-Fe_2O_3 dispersed in deionized water at pH 7.

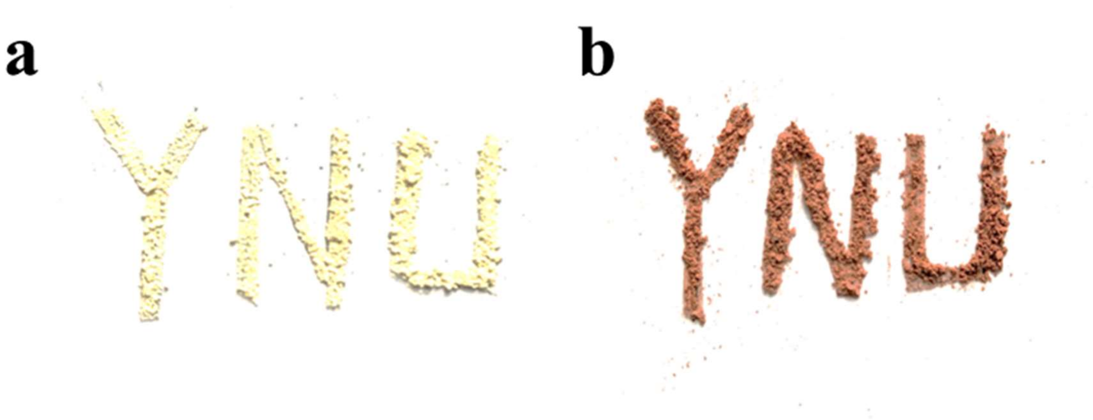

Figure S2. The sample patterns of g-C_3N_4 and Ag/α-Fe_2O_3/g-C_3N_4.

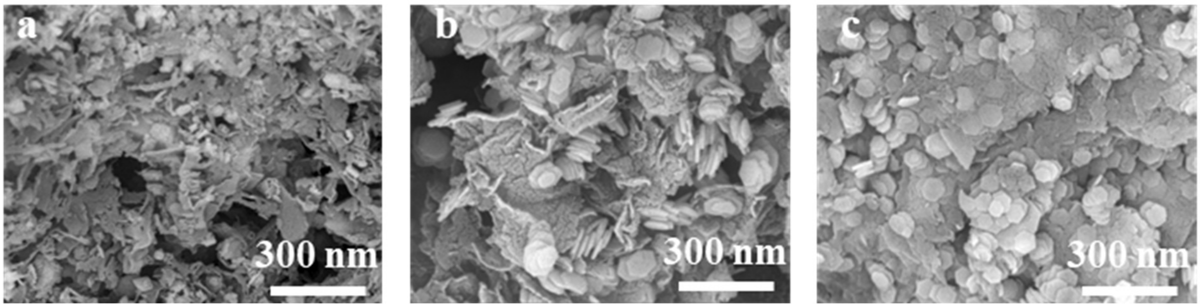

Figure S3. SEM images of α-Fe_2O_3/g-C_3N_4 for α-Fe_2O_3 weight ratios 20% (a), 30% (b), 40% (c).

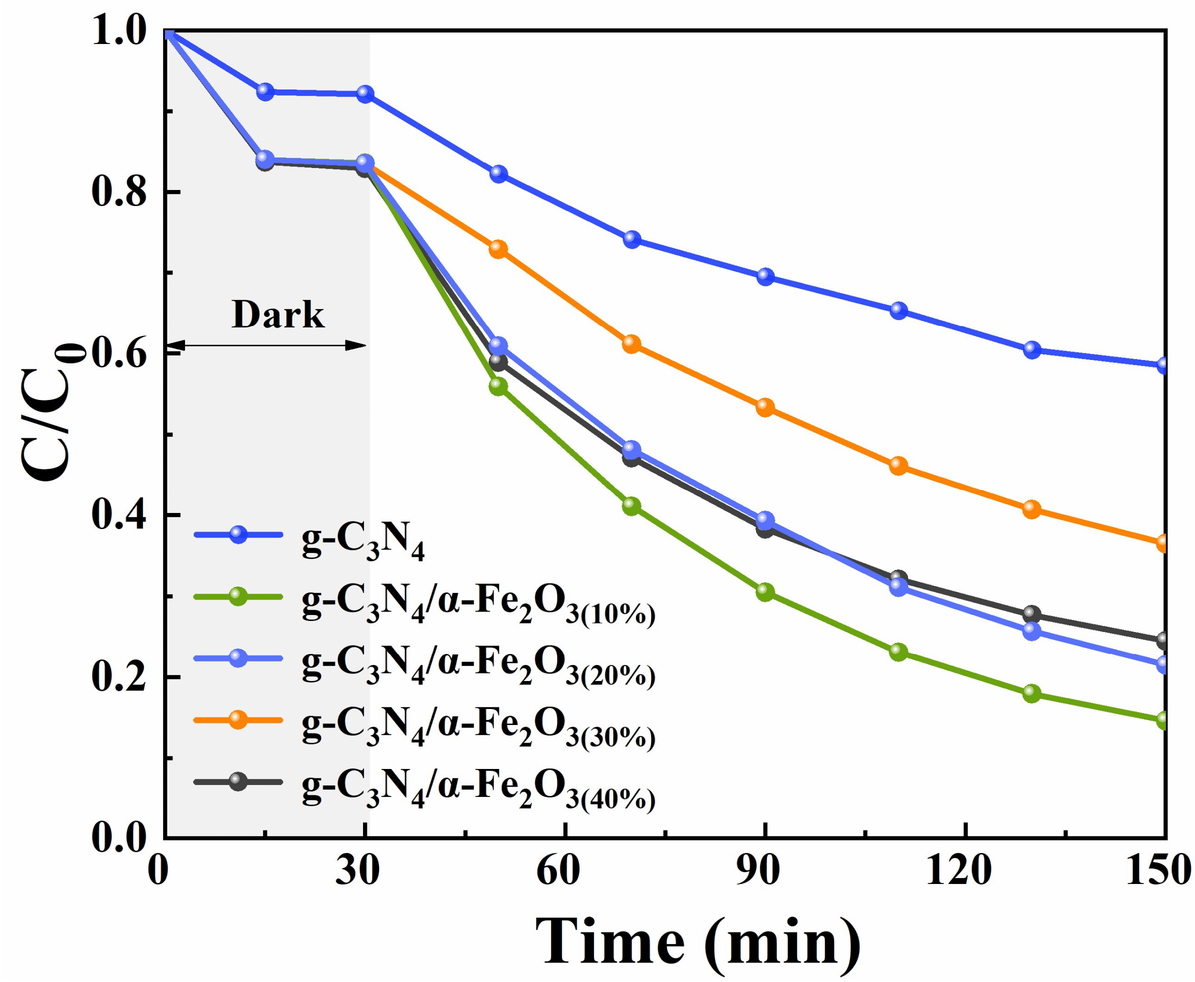

Figure S4. Degradation of TC by different weight ratios of α-Fe_2O_3/g-C_3N_4.

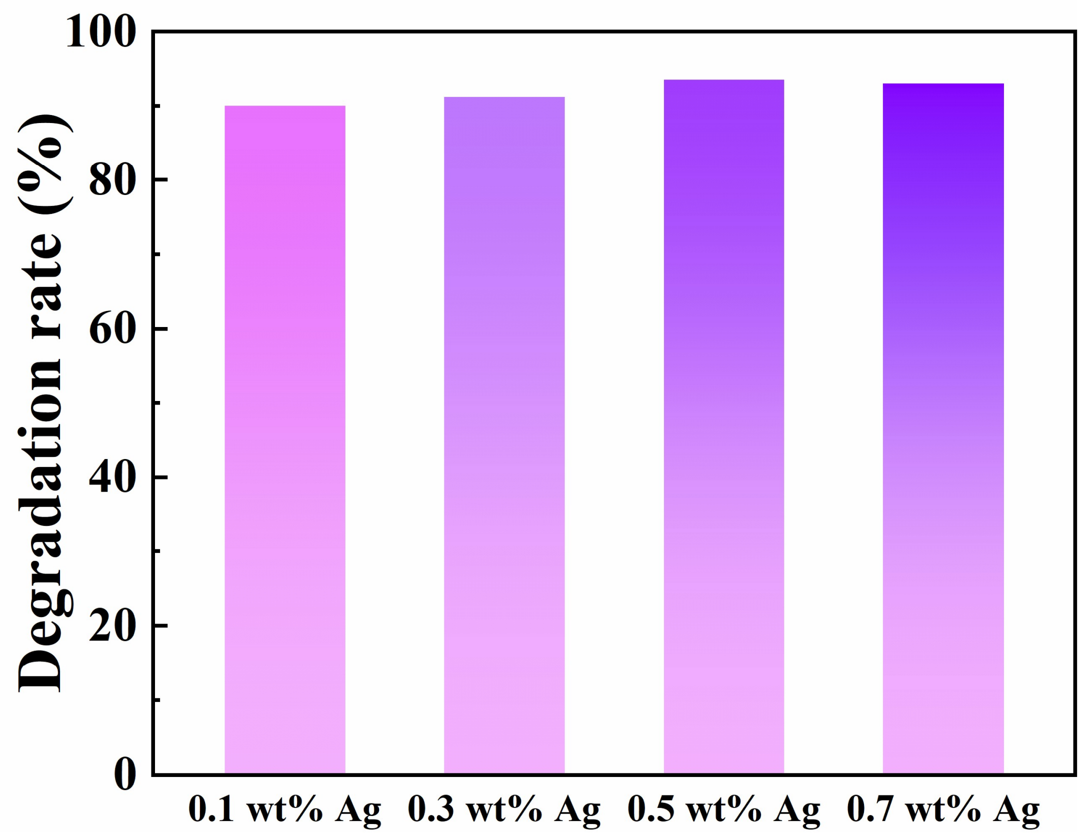

Figure S5. Degradation of TC by catalysts with different Ag loadings.

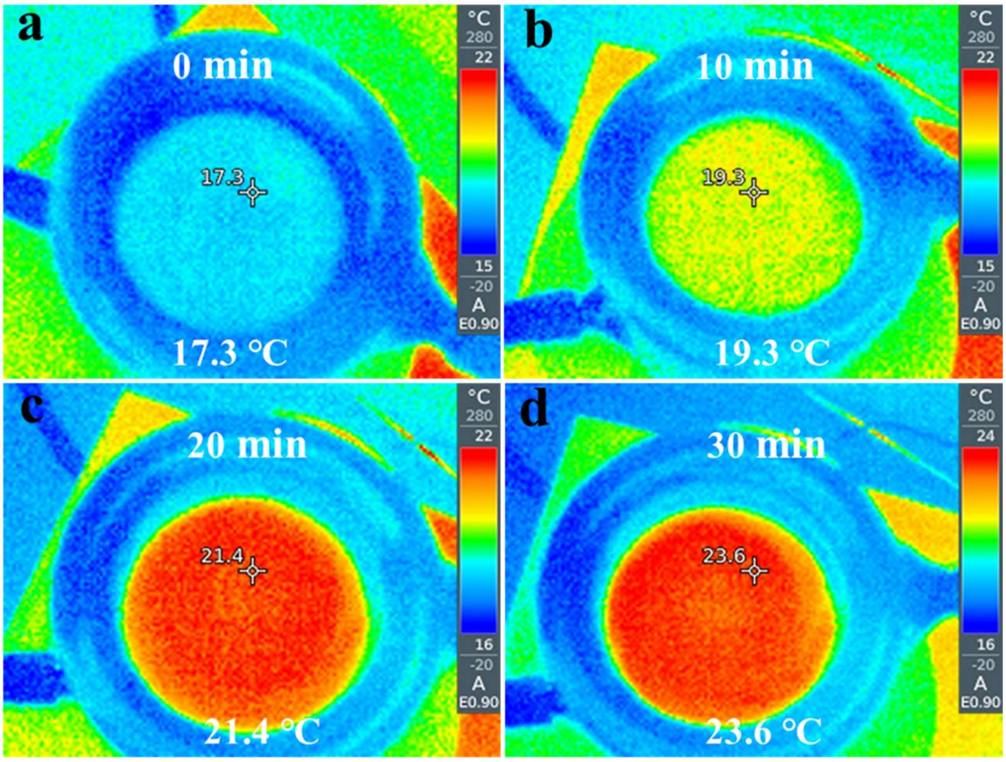

Figure S6. IR images of the pure water under illumination with a 300 w xenon lamp as a function of time.

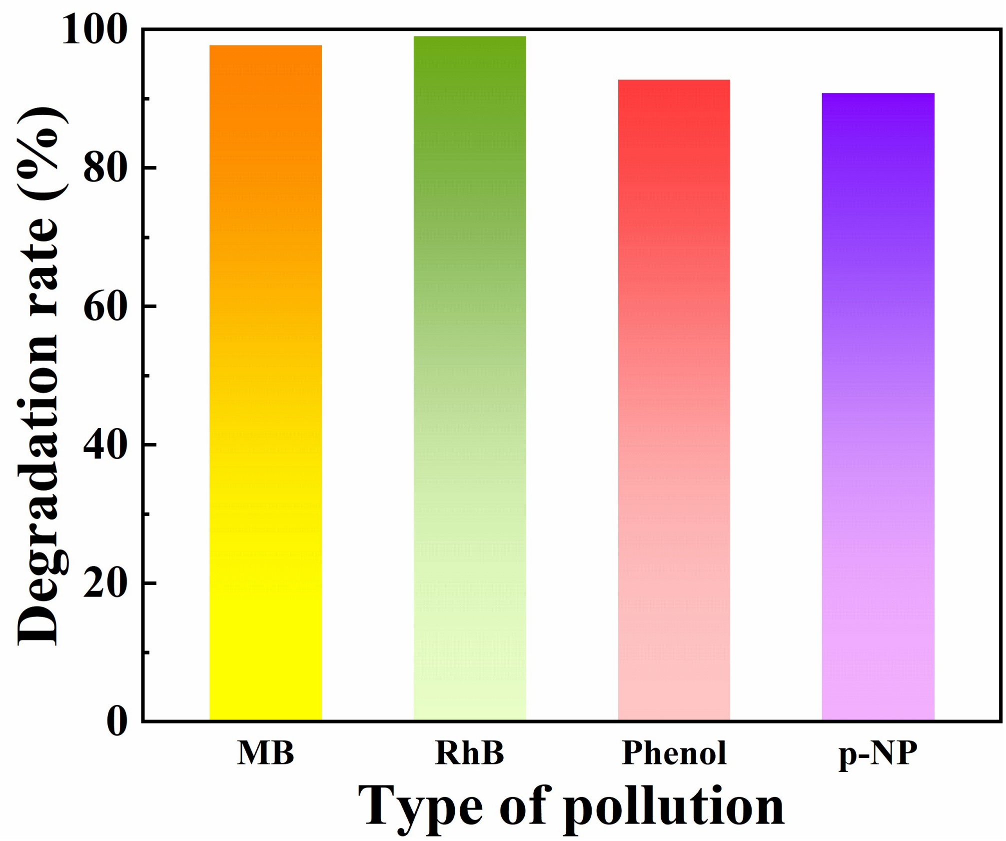

Figure S7. Photocatalytic degradation of other pollutants by Ag/α-Fe_2O_3/g-C_3N_4.

Table S1. Comparison of the performance of Ag/α-Fe_2O_3/g-C_3N_4 and other similar photocatalysts for H_2 evolution.

Photocatalysts	Light source	H_2 evolution rate (μmol g^{-1} h^{-1})	Ref.
Ag/α-Fe_2O_3/g-C_3N_4	**Xe lamp (300W)**	**3125**	**This work**
MoS_2/CdS/g-C_3N_4	300 W Xe lamp (λ>420 nm)	956	[8]
KCCN	Xe lamp (λ>420 nm)	557	[9]
α-Fe_2O_3/CdS/g-C_3N_4	Xe lamp (1000 W)	165	[10]
α-Fe_2O_3/g-C_3N_4(Pt)	Xe lamp (300W, λ>420 nm)	5000	[11]
$ZnIn_2S_4$/Ti_3C_2	Xe lamp (300 W, λ>420 nm)	979	[12]
g-C_3N_4/WO_3-carbon microsphere	Xe lamp (300W, λ > 420 nm)	2500	[13]
hollow core-shell TiO_2/g-C_3N_4	Xe lamp (300 w)	809	[14]

Table S2. Comparison of the photocatalytic performance of Ag/α-Fe_2O_3/g-C_3N_4 and other similar photocatalysts for TC degradation.

Photocatalysts	Light source	TC Removal rate	Ref.
Ag/α-Fe_2O_3/g-C_3N_4	**Xe lamp (300W, λ>420 nm)**	**93.6%**	**This work**
TiO_2-P25	Xe lamp (300 W, λ=350 nm)	94.8%	[1]
$CuInS_2$/Bi_2MoO_6	Xe lamp (300 W, λ>420 nm)	84.7%	[2]
Ag_2CO_3/$Bi_4O_5I_2$/g-C_3N_4	Xe lamp (300 W, λ>420 nm)	82.2%	[3]
β-Bi_2O_3@g-C_3N_4	Xe lamp (250 W, λ>420 nm)	80.2%	[4]
g-C_3N_4/ZrO_{2-x} NTs	Xe lamp (300 W, λ>420 nm)	90.6%	[5]
CDs/gC_3N_4/MoO_3	Xe lamp (350W, λ > 420 nm)	88.4%	[6]
g-C_3N_4/carbon nanotubes/$Bi_{25}FeO_{40}$	Xe lamp (500 w, λ > 420 nm)	87.9%	[7]

References

[1] Wu, S.; Hu, H.; Lin, Y.; Zhang, J; Hu. Y Visible light photocatalytic degradation of tetracycline over TiO_2. Chem. Eng. J. **2020**, 382, 122842.

[2] Guo, J.; Wang, L.; Wei, X.; Alothman, Z.; Albaqami, M.; Malgras, V.; Yamauchi, Y.; Kang, Y.; Wang, M.; Guan, W.; Xu, X. Direct Z-scheme $CuInS_2/Bi_2MoO_6$ heterostructure for enhanced photocatalytic degradation of tetracycline under visible light. J. Hazard. Mater. **2021**, 415, 125591.

[3] Chen, Z.; Guo, H.; Liu, H.; Niu, C.; Huang, D.; Yang, Y.; Liang, C.; Li, L.; Li, J. Construction of dual S-scheme $Ag_2CO_3/Bi_4O_5I_2$/g-C_3N_4 heterostructure photocatalyst with enhanced visible-light photocatalytic degradation for tetracycline. Chem. Eng. J. **2022**, 438, 135471.

[4] Hong, Y.; Li, C.; Yin, B.; Li, D.; Zhang, Z.; Mao, B.; Fan, W.; Gu, W.; Shi, W. Promoting visible-light-induced photocatalytic degradation of tetracycline by an efficient and stable beta-Bi_2O_3@g-C_3N_4 core/shell nanocomposite. Chem. Eng. J. **2018**, 338, 137-146.

[5] Chen, Q.; Yang, W.; Zhu, J.; Fu, L.; Li, D.; Zhou, L. Enhanced visible light photocatalytic activity of g-C_3N_4 decorated ZrO_{2-x} nanotubes heterostructure for degradation of tetracycline hydrochloride. J. Hazard. Mater. **2020**, 384, 121275.

[6] Xie, Z.; Feng, Y.; Wang, F.; Chen, D.; Zhang, Q.; Zeng, Y.; Lv, W.; Liu, G. Construction of carbon dots modified MoO_3/g-C_3N_4 Z-scheme photocatalyst with enhanced visible-light photocatalytic activity for the degradation of tetracycline. Appl. Catal. B: Environ. **2018**, 229, 96-104.

[7] Li, X.; Qiu, Y.; Zhu, Z.; Zhang, H.; Yin D. Novel recyclable Z-scheme g-C_3N_4/carbon nanotubes/$Bi_{25}FeO_{40}$ heterostructure with enhanced visible-light photocatalytic performance towards tetracycline degradation. Chem. Eng. J. **2022**, 429, 132130.

[8] Zhao, T.; Xing, Z.; Xiu, Z.; Li, Z.; Yang, S.; Zhou, W, Oxygen-doped MoS_2 nanospheres/CdS quantum dots/g-C_3N_4 nanosheets super-architectures for prolonged charge lifetime and enhanced visible-light-driven photocatalytic performance, ACS Appl. Mater. Interfaces, **2019**, 11, 7104-7111.

[9] Zhang, G.; Xu, Y.; Yan, D.; He, C.; Li, Y.; Ren, X.; Zhang, P.; Mi, H. Construction of k^+ ion gradient in crystalline carbon nitride to accelerate exciton dissociation and charge separation for visible light H_2 production, ACS Catal. **2021**, 11, 6995-7005.

[10] Yavuz, C.; Erten-Ela, S. Solar light-responsive α-Fe_2O_3/CdS/g-C_3N_4 ternary photocatalyst for photocatalytic hydrogen production and photodegradation of methylene blue. J. Alloys Compd. **2022**, 908, 164584.

[11] Li, Y.; Zhu, S.; Liang, Y.; Li, Z.; Wu, S.; Chang, C.; Luo, S.; Cui, Z. Synthesis of α-Fe_2O_3/g-C_3N_4 photocatalyst for high-efficiency water splitting under full light. Mater. Des. **2020**, 196, 109191.

[12] Huang, W.; Li, Z.; Wu, C.; Zhang, H.; Sun, J.; Li, Q. Delaminating Ti_3C_2 MXene by blossom of $ZnIn_2S_4$ microflowers for noble-metal-free photocatalytic hydrogen production. J Mater Sci Technol **2022**, 120, 89-98.

[13] Sun, M.; Zhou, Y.; Yu, T.; Wang J. Synthesis of g-C_3N_4/WO_3-carbon microsphere composites for photocatalytic hydrogen production. Int. J. Hydrog. Energy **2022**, 47, 10261-10276.

[14] Pan, J.; Dong, Z.; Wang, B.; Jiang, Z.; Zhao, C.; Wang, J.; Song, C.; Zheng, Y.; Li, C. The enhancement of photocatalytic hydrogen production via Ti^{3+} self-doping black TiO_2/g-C_3N_4 hollow core-shell nano-heterojunction. Appl. Catal. B: Environ. **2019**, 242, 92-99.